

## Analysis of the proximity effect and the interface transparency with perpendicular current in Ni/Nb system

S. Y. Huang, Y. C. Chiu, J. J. Liang, L. K. Lin, T. C. Tsai, S. Y. Hsu, and S. F. Lee

Citation: [Journal of Applied Physics](#) **105**, 07E319 (2009); doi: 10.1063/1.3073657

View online: <http://dx.doi.org/10.1063/1.3073657>

View Table of Contents: <http://scitation.aip.org/content/aip/journal/jap/105/7?ver=pdfcov>

Published by the [AIP Publishing](#)

---

### Articles you may be interested in

[Reentrant superconductivity and superconducting critical temperature oscillations in F/S/F trilayers of Cu<sub>41</sub>Ni<sub>59</sub>Nb/Cu<sub>41</sub>Ni<sub>59</sub> grown on cobalt oxide](#)

*J. Appl. Phys.* **114**, 033903 (2013); 10.1063/1.4813131

[Proximity effect in Nb-Mo layered films: Transition temperature and critical current dependence on period](#)

*J. Appl. Phys.* **110**, 073916 (2011); 10.1063/1.3650239

[Proximity effect on vortex dynamics at low field in Nb and Nb/Au bilayer microbridges exhibiting strong pinning](#)

*J. Appl. Phys.* **110**, 063919 (2011); 10.1063/1.3636111

[Proximity effect and interface transparency in Nb/Cu multilayers](#)

*J. Appl. Phys.* **106**, 113917 (2009); 10.1063/1.3267868

[Planar S-\(S/F\)-S Josephson junctions induced by the inverse proximity effect](#)

*Appl. Phys. Lett.* **95**, 062501 (2009); 10.1063/1.3200226

---



## Re-register for Table of Content Alerts

Create a profile.



Sign up today!



## Analysis of the proximity effect and the interface transparency with perpendicular current in Ni/Nb system

S. Y. Huang,<sup>1,2</sup> Y. C. Chiu,<sup>1</sup> J. J. Liang,<sup>3</sup> L. K. Lin,<sup>1</sup> T. C. Tsai,<sup>1</sup> S. Y. Hsu,<sup>2</sup> and S. F. Lee<sup>1,a)</sup>

<sup>1</sup>*Institute of Physics, Academia Sinica, Taipei, Taiwan 115, Republic of China*

<sup>2</sup>*Institute of Electrophysics, National Chiao-Tung University, Hsinchu, Taiwan 300, Republic of China*

<sup>3</sup>*Department of Physics, Fu Jen Catholic University, Taipei, Taiwan 242, Republic of China*

(Presented 13 November 2008; received 18 September 2008; accepted 28 November 2008; published online 11 March 2009)

We quantitatively study the interface resistance in Ni/Nb multilayers fabricated by sputtering system. For a fixed Ni layer thickness in Ni/Nb/Ni trilayers, the superconducting temperature  $T_c$  decreases with decreasing Nb thickness. By analyzing the data with the proximity effect, the critical thickness below which superconductivity vanished was deduced. From current perpendicular to plane (CPP) measurement interpreted with a one-band series-resistor model, we obtained the CPP resistivities of Nb and Ni and the unit area resistances of  $4.2 \pm 0.2$  and  $1.5 \pm 0.4$   $\mu\Omega$   $m^2$  for superconducting and normal Ni/Nb interfaces. The transparency parameter is directly calculated in terms of interface resistance. © 2009 American Institute of Physics. [DOI: 10.1063/1.3073657]

Rich interesting phenomena have been found in hybrids of superconductors ( $S$ ) and ferromagnets ( $F$ ) due to the proximity effect between competing orders in the interface. The  $S$  prefers an antiparallel spin orientation in Cooper pairs, while the  $F$  forces the spins to align in parallel by exchange force. Many studies have been devoted to investigate both fundamental and applicative aspects of this unusual research field.<sup>1</sup> However, only recently the quality of the interface has been added to model the interaction between the  $S$  and  $F$  layers. An important parameter of interface transparency,  $\gamma_b$ , has been used to describe the role of the boundary condition among different layers depending on interface imperfections, Fermi velocities, and band structure mismatch.<sup>2</sup> Here  $\gamma_b$  is defined as the ratio of interface resistance to the product of resistivity and the Cooper pair penetration depth in the  $F$ . It is usually treated as an adjustable parameter due to difficulty in direct measurements.<sup>3</sup> Recently, the interface resistances,  $AR$  (area  $A \times$  resistance  $R$ ), for both lattice-matched and lattice-mismatched pairs have become feasible to be calculated with no free parameters.<sup>4</sup> We study the proximity effect between fcc Ni and bcc Nb with mismatched lattice constant about 6.7%. Current perpendicular to plane (CPP) measurement is used to determine the interface resistance between Ni and Nb in both superconducting and normal states. The quantitative values of  $AR_{Ni/Nb}$  obtained from the current work allow us to determine the interface transparency of the Ni layer without introducing any arbitrary fitting parameter.

Samples were fabricated on Si (100) substrates without breaking the vacuum during the dc magnetron sputtering so that samples are of comparable interface quality. The details of sample preparation, sample geometry, and measuring techniques were reported in Ref. 5. The superconducting critical temperature  $T_c$  is determined from resistance measurement using a standard four-probe technique with current

flowing in the layer plane. Figure 1 shows the  $T_c$  for Ni/Nb/Ni trilayers as a function of Nb thickness. For CPP cause, the sample is sandwiched between two circular Nb electrodes in order for the current uniformly flowing through the whole sample. In the inset of Fig. 2 is the top view geometry of CPP configuration where the top and bottom Nb strips are used for the four-point measurement. Each Nb strip and circular electrode is 200 nm thick in order to superconduct at the measuring temperature of 4.2 K. The total thickness and sample area  $A$  were verified with a stylus surface profiler.

The resistivities of bulk Nb and Ni, thicker than 500 nm, were 8 and 4  $\mu\Omega$  cm at 10 K. However, the low-temperature resistivity of the film drastically increased with reducing thickness, as shown in the inset of Fig. 1. The thickness dependence of pure Ni resistivity could be described by the

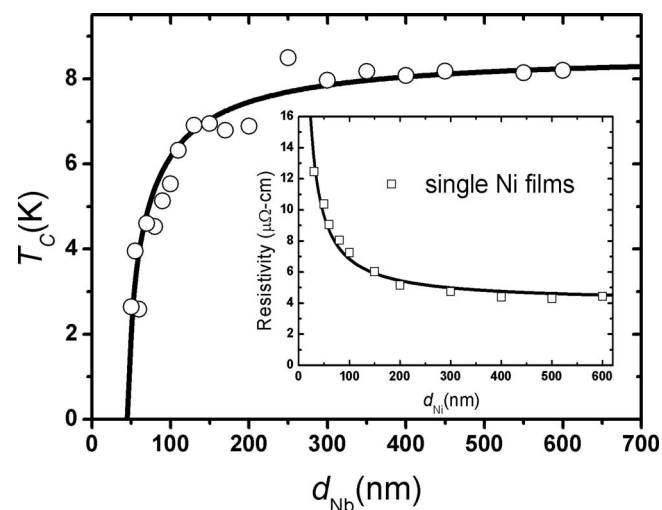


FIG. 1. The superconducting critical temperatures for Ni/Nb/Ni trilayers as a function of  $d_{Nb}$ . The solid line is obtained from the theoretical fitting with parameters of  $\xi_S=19$  nm and  $\gamma=0.1$ . Inset: Thickness dependence of the low-temperature resistivity as a function of the single Ni layer fitted by the Fuchs-Sondheimer relation.

a)Electronic mail: leesf@phys.sinica.edu.tw.

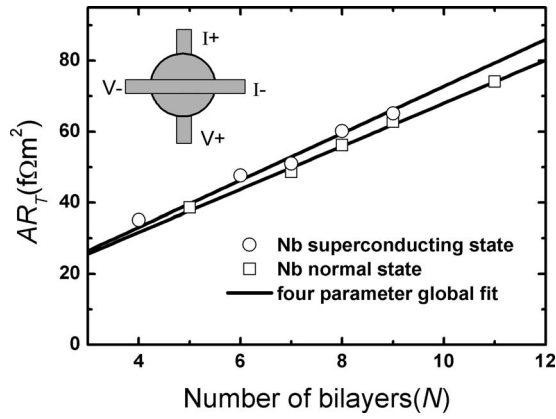


FIG. 2. Unit area resistance,  $AR_T$ , vs bilayer number  $N$  measured at 4.2 K. The two sets of samples have Nb thicknesses fixed at 12 and 108 nm, respectively. The solid lines are global fits for four parameters to the data. Inset: The top view geometry of the CPP configuration. Sample is sandwiched between the two circular Nb electrodes. The top and bottom Nb strips are used for the four-point measurement.

Fuchs–Sondheimer relation  $\rho(d) = \rho_B [1 + (3l/8d)]$ , where  $\rho_B$  is the bulk resistivity.<sup>6</sup> The fit yields  $\rho_B = 4 \mu\Omega \text{ cm}$  and the mean free path  $l$  about 180 nm. The  $T_c$  for Ni(50 nm)/Nb( $d_S$ )/Ni(50 nm) trilayers as a function of Nb layer thickness is shown in Fig. 1. The monotonically rapid reduction in  $T_c$  down to a critical thickness,  $d_{\text{crit}}$ , results from the pair-breaking effect that suppresses the amplitude of the superconducting wave function near the  $F/S$  interface. The microscopically theoretical model we used to describe the dependence  $T_c(d_{\text{Nb}})$  for the Ni/Nb/Ni trilayer is based on Usadel equation which has been proposed by Radović *et al.*<sup>7</sup> In the single-mode approximation, the decrease in  $T_c$  is related to the effective pair-breaking  $\eta$  parameter by

$$\ln\left(\frac{T_c}{T_{c0}}\right) = \Psi\left(\frac{1}{2}\right) - \text{Re} \Psi\left(\frac{1}{2} + \frac{\eta}{T_c T_{c0}}\right),$$

$$K_s d_s \tan\left(\frac{K_s d_s}{2}\right) = 2(1+i)\gamma \frac{d_s}{\xi_S} \tanh\left[2(1+i)\frac{d_F}{\xi_F}\right], \quad (1)$$

with  $\gamma = \rho_S \xi_S / \rho_F \xi_F$  which can be taken as the strength of the proximity effect between the  $F$  and  $S$  metals. Here  $\xi_F = \sqrt{4\hbar D_{FM}/I_0}$  is the penetration length of the Cooper pair into ferromagnet and  $\xi_S$  is the coherence length of superconductor.  $I_0$  is the spin splitting energy of  $F$ , and  $D_F = (1/3\gamma_F \rho_F)(\pi k_B/e)^2$  is the diffusion constant with the electronic specific heat coefficient  $\gamma_F$  in the  $F$  layer. The  $\text{Re} \Psi$  represents the real part of the digamma function,  $T_{c0}$  is the bulk critical temperature, and  $K_s$  is the propagation momentum. The  $I_0 \approx 100 \text{ meV}$  for Ni,<sup>8</sup>  $\gamma_F \approx 7.02 \times 10^{-3} \text{ J/K}^2 \text{ mol}$ ,<sup>9</sup> and  $\xi_F \approx 4.1 \text{ nm}$  are input parameters to model  $T_c(d_F)$ . Due to the fact that Ni has smaller splitting energy,  $\xi_F \approx 4.1 \text{ nm}$  is longer than the values  $\xi_{\text{Fe}} \approx 1.2 \text{ nm}$  and  $\xi_{\text{Co}} \approx 1.3 \text{ nm}$  obtained in Fe/Nb/Fe (Ref. 10) and Co/Nb/Co (Ref. 11) trilayers, respectively. A good fit for  $\xi_S \approx 19 \text{ nm}$  and  $\gamma \approx 0.1$  is shown as a solid line in Fig. 1. Moreover, it gives a critical thickness  $d_{\text{crit}}(\text{Ni}) = 45 \text{ nm}$  by extrapolating the fit to  $T_c = 0$ .

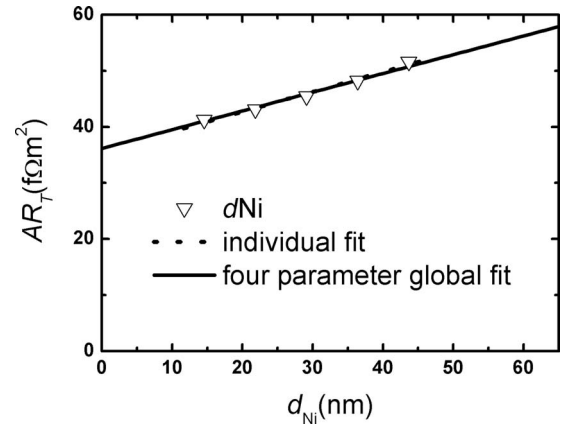


FIG. 3. Unit area resistance,  $AR_T$ , vs Ni thickness with Nb thickness fixed at 27 nm and  $N=7$  measured at 4.2 K. The dashed line is linear least-squares fit. The solid line is global fit for four parameters to the data.

According to this phase diagram, when the Nb thickness was thinner than  $d_{\text{crit}}$ , we had  $N/F$  system; when Nb was thicker, we had  $S/F$  systems. In the present study, four series of CPP samples were made:

1. Ni(58 nm)/[Nb(108 nm)/Ni(58 nm)] $_N$  with varying numbers of bilayers for superconducting state Nb;
2. Ni(78 nm)/[Nb(12 nm)/Ni(78 nm)] $_N$  with varying numbers of bilayers for normal state Nb;
3. Ni( $d_{\text{Ni}}$ )/[Nb(27 nm)/Ni( $d_{\text{Ni}}$ )] $_7$  with seven bilayers and varying Ni thicknesses; and
4. Ni(78 nm)/[Nb( $d_{\text{Nb}}$ )/Ni(78 nm)] $_7$  with seven bilayers and varying Nb thicknesses.

Figure 2 presents the total resistance  $AR_T$ , the unit area resistance on multilayer, versus bilayer number,  $N$ , for the first two series of samples. The  $AR_T$  is linearly proportional to the number of bilayers for Nb both in the normal and superconducting states. Since there is no exchange coupling between Ni and Nb films, a one-band model could be sufficient to describe the linear behavior of  $AR_T$  versus  $N$  as follows:

$$AR_T = 2AR_{F/S(S)} + \rho_F t_F + N(\rho_F t_F + \rho_S t_S + 2AR_{F/S(NM)}) \quad (2)$$

for normal Nb and

$$AR_T = 2AR_{F/S(S)} + \rho_F t_F + N(\rho_F t_F + 2AR_{F/S(S)}) \quad (3)$$

for superconducting Nb.

Here  $t$ 's are the thicknesses and  $AR_{F/S(NM),(S)}$ 's are the interface resistances between Ni and Nb layers for normal and superconducting states, respectively. From the series 3 and 4, the CPP resistivities could be determined by measuring the CPP resistance with varying layer thicknesses of Nb and Ni. Figures 3 and 4 show the  $AR_T$  behavior as a function of Ni and Nb thicknesses, respectively, for  $d_{\text{Nb}}$  smaller than  $d_{\text{crit}}(\text{Ni})$  and seven bilayers. Following Ohm's law, the total resistance is proportional to the thickness. For the Nb and Ni resistivities are independent of the layer thickness, the one-band model gives the linear behavior of  $AR_T$  versus thickness as

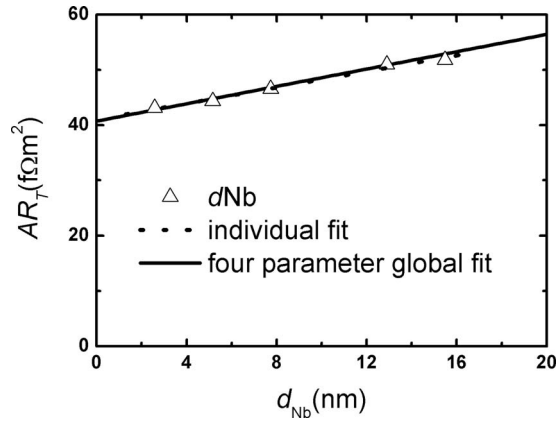


FIG. 4. Unit area resistance,  $AR_T$ , vs Nb thickness with Ni thickness fixed at 78 nm and  $N=7$  measured at 4.2 K. The dashed line is linear least-squares fit. The solid line is global fit for four parameters to the data.

$$AR_T = 2AR_{F/S(S)} + 14AR_{F/S(NM)} + 7\rho_S t_S + 8\rho_F d_F \quad (4)$$

for varying Ni thicknesses with Nb thickness fixed at 27 nm and

$$AR_T = 2AR_{F/S(S)} + 14AR_{F/S(NM)} + 7\rho_S d_S + 8\rho_F t_F \quad (5)$$

for varying Nb thicknesses with Ni thickness fixed at 78 nm. The individual linear least-squares fits of  $AR_T$  versus  $d_{Ni}$  and  $d_{Nb}$  yield slopes  $\rho_{Ni}$  of 4.5 and  $\rho_{Nb}$  of 10  $\mu\Omega$  cm and are plotted as dashed lines in Figs. 3 and 4, respectively. Even though each series of samples could be individually fitted with the model, there is mutual uncertainty between different sets, as reported earlier.<sup>5</sup> Since the four sets of data share the same parameters, we treat all resistivities and the interface resistance as fitting parameters to perform the four-parameter global fit. The solid lines in Figs. 2–4 are the best global fits for four parameters to all data and give  $\rho_{Ni} = 4.2 \pm 0.3 \mu\Omega$  cm,  $\rho_{Nb} = 11 \pm 1.0 \mu\Omega$  cm,  $2AR_{Ni/Nb(NM)} = 1.5 \pm 0.4 \text{ f}\Omega \text{ m}^2$ , and  $2AR_{Ni/Nb(S)} = 4.2 \pm 0.2 \text{ f}\Omega \text{ m}^2$ . The latter value is within experimental error of  $4.8 \pm 0.6 \text{ f}\Omega \text{ m}^2$  that was reported by Fierz *et al.*<sup>12</sup> The transparency parameter was then calculated with  $\gamma_b = (AR_{F/S(NM)} / \rho_F \xi_F^*)$  without spin-flip scattering, where  $AR_{F/S(NM)}$  is the unit area resistance at normal state and  $\rho_F$  is the resistivity of  $F$ .  $\xi_F^* = \sqrt{\hbar D_F / 2\pi K_B T_C}$  is the penetration length which corresponds to the actual penetration depth of the Cooper pairs in the  $F$  without considering the exchange field. We deduced the  $\gamma_b = 2.0$  for Ni/Nb as  $S$  is in the normal state.

When Nb is in the superconducting state, the  $AR_{Ni/Nb(S)}$  is larger than  $AR_{Ni/Nb(NM)}$  in the Ni/Nb system. A spin-up electron injected from a normal metal is retroreflected at the interface as a spin-down hole in order to form a Cooper pair in the  $S$  which is described as the Andreev reflection.<sup>13</sup> If the normal metal is replaced by  $F$ , the Andreev current at the  $S/F$  interface is partially suppressed by the exchange splitting of the conduction band in the ferromagnet. Moreover, the spin accumulation in the boundary of  $F$  leads to an additional voltage drop across the interface due to reduced spin transport into  $S$ . These would be the main factor for the interface resistance of Ni/Nb larger in the superconducting state than in the normal state.

In summary, the critical thickness in the Ni/Nb/Ni trilayer structure has been derived within the framework of proximity theory. We have presented the values of interface resistance from CPP measurement by the one-band model with the best fit. The unit area resistances of one pair of the Ni/Nb interface are  $1.5 \pm 0.4$  and  $4.2 \pm 0.2 \text{ f}\Omega \text{ m}^2$  at normal and superconducting Nb states, respectively. The interface transparency can be directly extracted from the interface resistance. Our results are important for understanding complex interfacial transport for the  $F/S$  heterostructures.

The financial support of Academia Sinica and National Science Council of Taiwan, Republic of China is acknowledged.

<sup>1</sup>A. I. Buzdin, *Rev. Mod. Phys.* **77**, 935 (2005).

<sup>2</sup>*Nanoscale Devices—Fundamentals and Applications*, edited by R. Gross, A. Sidorenko, and L. Tagirov (Springer, New York, 2006), pp. 241–249.

<sup>3</sup>Ya. V. Fominov, N. M. Chchelkatchev, and A. A. Golubov, *Phys. Rev. B* **66**, 014507 (2002).

<sup>4</sup>P. C. Xu and K. Xia, *Phys. Rev. B* **74**, 184206 (2006).

<sup>5</sup>S. Y. Huang, S. F. Lee, S. Y. Hsu, and Y. D. Yao, *Phys. Rev. B* **76**, 024521 (2007).

<sup>6</sup>E. H. Sondheimer, *Phys. Rev.* **80**, 401 (1950).

<sup>7</sup>Z. Radović, M. Ledvij, L. Dobrosavljević-Grujić, A. I. Buzdin, and J. R. Clem, *Phys. Rev. B* **44**, 759 (1991).

<sup>8</sup>J. W. A. Robinson, S. Piano, G. Burnell, C. Bell, and M. G. Blamire, *Phys. Rev. B* **76**, 094522 (2007).

<sup>9</sup>C. Kittel, *Introduction to Solid State Physics* (Wiley, New York, 1986), p. 144.

<sup>10</sup>S. Y. Huang, S. F. Lee, J. J. Liang, C. Y. Yu, K. L. You, T. W. Chiang, S. Y. Hsu, and Y. D. Yao, *J. Magn. Magn. Mater.* **304**, e81 (2006).

<sup>11</sup>J. J. Liang, S. F. Lee, W. T. Shih, W. L. Chang, C. Yu, and Y. D. Yao, *J. Appl. Phys.* **92**, 2624 (2002).

<sup>12</sup>C. Fierz, S. F. Lee, J. Bass, W. P. Pratt, Jr., and P. A. Schroeder, *J. Phys.: Condens. Matter* **2**, 9701 (1990).

<sup>13</sup>G. E. Blonder, M. Tinkham, and T. M. Klapwijk, *Phys. Rev. B* **25**, 4515 (1982).